

Adsorption of finite semiflexible polymers and their loop and tail distributions

Tobias A. Kampmann* and Jan Kierfeld†

Physics Department, TU Dortmund University, 44221 Dortmund, Germany

(Dated: June 20, 2018)

We discuss the adsorption of semiflexible polymers to a planar attractive wall and focus on the questions of the adsorption threshold for polymers of *finite* length and their loop and tail distributions using both Monte-Carlo simulations and analytical arguments. For the adsorption threshold, we find three regimes: (i) a flexible or Gaussian regime if the persistence length is smaller than the adsorption potential range, (ii) a semiflexible regime if the persistence length is larger than the potential range, and (iii) for finite polymers, a novel crossover to a rigid rod regime if the deflection length exceeds the contour length. In the flexible and semiflexible regime, finite size corrections arise because the correlation length exceeds the contour length. In the rigid rod regime, however, it is essential how the global orientational or translational degrees of freedom are restricted by grafting or confinement. We discuss finite size corrections for polymers grafted to the adsorbing surface and for polymers confined by a second (parallel) hard wall. Based on these results we obtain a method to analyze adsorption data for finite semiflexible polymers such as filamentous actin. For the loop and tail distributions, we find power laws with an exponential decay on length scales exceeding the correlation length. We derive and confirm the loop and tail power law exponents for flexible and semiflexible polymers. This allows us to explain that, close to the transition, semiflexible polymers have significantly smaller loops and both flexible and semiflexible polymers desorb by expanding their tail length. The tail distribution allows us to extract the free energy per length of adsorption for actin filaments from experimental data [D. Welch *et al.*, *Soft Matter* **11**, 7507 (2015)].

I. INTRODUCTION

For semiflexible polymers their intrinsic bending energy associated with their bending rigidity κ is relevant for shape fluctuations. The competition between thermal and bending energy determines the persistence length $L_p \sim \kappa/k_B T$ of the polymer, which is the decay length of orientational correlations along a free polymer. For semiflexible polymers the persistence length is large and comparable to other length scales in the problem. Examples of semiflexible polymers are stiff synthetic polymers such as polyelectrolytes [1, 2] and many stiff biopolymers such as DNA, filamentous (F-)actin, or microtubules. The persistence length of F-actin is in the $10 \mu\text{m}$ -range [3] and ranges up to the mm-range for microtubules [4]. The bending rigidity also modifies the adsorption behavior of semiflexible polymers. In a recent experiment [5], the conformations of single, finite actin filaments adsorbed onto a planar wall by a depletion interaction have been analyzed and compared with Monte-Carlo simulations based on a phenomenological treatment of finite size effects. In this paper we want to go beyond the analysis given in Ref. 5 and systematically derive a procedure to analyze finite size effects for semiflexible polymer adsorption.

The adsorption of single flexible polymer chains has been extensively studied theoretically (see, for example, Refs. 6–8). Theoretical studies on the adsorption of semiflexible polymers with intrinsic bending stiffness are less but still numerous [2, 5, 9–27] and fall into

two main classes, which are studies of lattice polymers [9, 13, 15, 24, 27] or of off-lattice continuous polymers [2, 5, 10–12, 14, 16–21, 23, 25, 26]; in Ref. 22, only the binding potential was realized in a discrete manner by explicitly discrete pinning sites. We will conduct off-lattice simulations and exact off-lattice calculations in the rigid rod limit. In order to quantify loop and tail distributions we use critical exponent relations based on necklace model [28] and transfer matrix approaches for off-lattice polymers. Closely related to adsorption is the conformational statistics of semiflexible polymers confined to the half-plane [29] and slits or channels [30–36], from which we will also use concepts such as the deflection length and exact results on critical exponents.

From a theoretical point of view, the adsorption of semiflexible polymers is challenging because it involves several competing length scales. For a freely fluctuating semiflexible polymer, the persistence length L_p and its contour length L are the relevant length scales. For $L \lesssim L_p$, thermal fluctuations are dominated by bending energy. This is the regime we will mostly focus on in this work and which is relevant for actin filaments, where typically both L and L_p are in the range of $10 - 20 \mu\text{m}$. For $L \lesssim L_p$ the bending energy will also suppress self-intersections and, thus, effects from self-avoidance. If $L \ll L_p$, the semiflexible polymer approaches a rigid rod. For $L \gg L_p$, on the other hand, the polymer is well-described by a flexible polymer with an effective segment length $\sim L_p$. In the adsorption problem, both L and L_p also compete with the correlation length ξ of the adsorption transition and the range ℓ of the adsorption potential.

For the adsorption transition, polymers longer than the correlation length, $L \gg \xi$, can be regarded as quasi-infinite. Then the correlation length ξ is the character-

* tobias.kampmann@udo.edu

† jan.kierfeld@tu-dortmund.de

istic maximal length of desorbed segments (loops and tails) and diverges at the adsorption transition. If the persistence length is small compared to the correlation length, $L_p < \xi$, the critical exponents of the adsorption transition cross over to those of a flexible polymer, if self-avoidance is taken into account to those of a flexible self-avoiding chain. For semiflexible polymers with large L_p , this crossover can only be observed very close to the adsorption transition [10, 23]. We will show that the crossover from semiflexible to flexible critical behavior is also reflected in the length distribution of the desorbed loops or tails. We find different exponents for loop and tail distributions of flexible and semiflexible polymers, which give rise to a different desorption behavior: semiflexible polymers have significantly smaller loops closed to the transition but both flexible and semiflexible polymers desorb by expanding the tail. This explains previous observations in simulations [5, 27].

The critical potential strength itself is, however, to leading order, the critical potential strength to adsorb single segments of size L_p and, thus, mainly determined by semiflexible fluctuations on scales $< L_p$ [23]. Flexible behavior only occurs if the persistence length becomes smaller than the adsorption potential range, $L_p < \ell$ [25, 26]. This can be qualitatively understood from the simple argument that adsorption of individual segments of length L_p is a necessary condition for the adsorption of the entire chain. The result is in accordance with simulation results on the adsorption threshold, which can be well explained using semiflexible polymer theory [26] regardless of whether $\xi < L_p$ or $\xi > L_p$ as long as only $L_p \gg \ell$, i.e., the semiflexible polymer is sufficiently rigid that its persistence length remains large compared to the potential range ℓ and loop formation of adsorbed trains inside the adsorption potential remain suppressed.

According to the theory of phase transitions, finite size effects will modify the adsorption behavior close to the transition if $L < \xi$ such that the length of desorbed loops or tails is limited by the finite polymer length.

For finite stiff polymers, we find a novel rigid rod regime with qualitatively different finite size effects. In the rigid rod regime, it is essential how the global orientation degrees of freedom are restricted by grafting or confinement. Finite size effects then crucially depend on Odijk's deflection length

$$L_d \sim L_p^{1/3} \ell^{2/3}, \quad (1)$$

which is the length scale for collisions of the adsorbed polymer with the boundaries of a potential well of width ℓ [30]. A finite stiff polymer with the deflection length L_d exceeding its length L , effectively behaves as a weakly fluctuating rigid rod. We will show that finite size effects are then governed by the global orientation of the weakly fluctuating rod if it is end-grafted to the adsorbing surface. For a stiff polymer confined by a second wall to the adsorbing surface, also the global translation degree of freedom becomes relevant. For a flexible polymer, on the other hand, there is no preferred orientation of the

	$L_p < \ell$	$L_p > \ell$	$L_d > L$
$L > \xi, L_d$	flexible, infinite	semiflexible, infinite	n.a.
$L < \xi$	flexible, fin. size effect	semiflexible, fin. size effects	finite rigid rod

TABLE I Different regimes for the adsorption threshold of a continuous semiflexible polymer. The critical exponents should cross over from semiflexible to flexible (or self-avoiding flexible) for $\xi > L_p$ close to the desorption threshold. In addition, for a semiflexible chain with bond length b , discretization effects occur for $b > L_d$.

polymer, which is thus irrelevant for finite size scaling.

The different regimes for the adsorption threshold are summarized in table I and illustrated by simulation snapshots in Fig. 1. Understanding the influence of global degrees of freedom on finite size effects for stiff polymers is important to correctly analyze adsorption data for finite semiflexible polymers. For decreasing stiffness such that $L_d \ll L$, internal deformation degrees of freedom dominate, and there is a crossover from the novel rigid rod regime to the standard finite size corrections from a correlation length growing beyond the contour length, $\xi > L$. From these results we can derive a procedure to analyze finite size effects for semiflexible polymer adsorption in simulations or for example, in the experimental data of Ref. 5 on the adsorption of filamentous actin.

The paper is organized as follows. In Sec. II, we introduce the theoretical and Monte-Carlo simulation model for the adsorption of semiflexible polymers on a planar substrate. Then, we briefly recapitulate results on the adsorption threshold of infinite semiflexible polymers. Afterwards, the loop and tail distributions close to the adsorption transition are derived and used to extract the free energy of adsorption from measured adsorption data. We then focus on the adsorption threshold for *finite* semiflexible polymers and obtain a complete picture featuring a flexible, a semiflexible and a novel rigid rod regime. We consider different adsorption geometries, in particular, we compare end-grafted semiflexible polymers and semiflexible polymers confined between two walls. Finally, our results lead to a method to analyze adsorption data for finite semiflexible polymers such as filamentous actin. We conclude with a discussion of experimental realizations.

II. MODEL AND SIMULATION

We use the same semiflexible polymer model as in Ref. 26 and start from a continuum worm-like chain model for a polymer contour $\mathbf{r}(s)$ of length L parameterized by its arc length s ($0 < s < L$). Its energy consists of a bending energy $\mathcal{H}_b[\mathbf{r}(s)] = \int_0^L ds \frac{\kappa}{2} (\partial_s^2 \mathbf{r})^2$ and an adsorption energy $\mathcal{H}_{ad}[\mathbf{r}(s)] = \int_0^L ds V(z(s))$ in an external potential

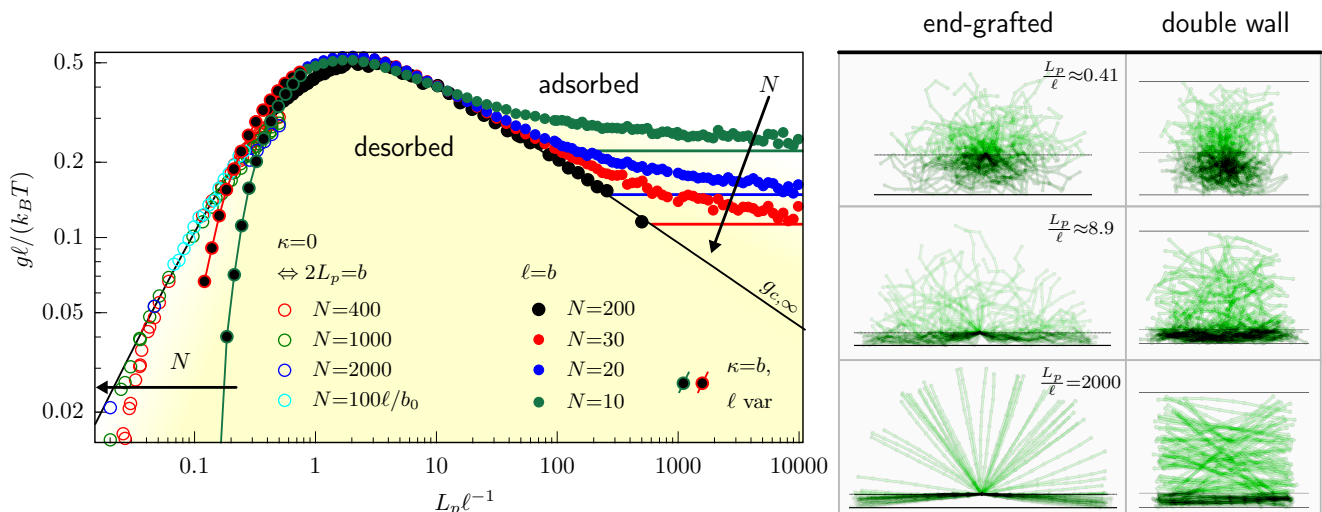


FIG. 1 Simulation data for the adsorption threshold g_c of finite end-grafted polymers as a function of dimensionless polymer stiffness L_p/ℓ and three snapshots for different stiffness illustrating the three regimes of flexible, semiflexible and rigid rod adsorption. We also show the corresponding snapshots for polymers confined between two walls (see also Fig. 7 below for the simulation results on the adsorption threshold). The snapshots show barely adsorbed ($g \gtrsim g_c$, $N = 10$) polymers and are taken in two dimensions for clarity, whereas all simulations in this paper were performed in $D=3$. To illustrate typical configurations, each snapshot shows several (> 100) configurations. We use the maximum of the cumulant $C_{\text{ad}} = \langle L_{\text{ad}}^2 \rangle - \langle L_{\text{ad}} \rangle^2$ to determine the adsorption threshold g_c numerically. For the stiffer chains (Filled colored circles, $L_p/\ell > 1$) we vary L_p and for more flexible chains (Colored circles with black filling, $L_p/\ell < 1$) we vary ℓ . Additionally, we simulate chains without bending stiffness $\kappa=0$, where the persistence length is $2L_p=b$ according to the Kuhn length (colored open circles). In the stiff regime, horizontal lines indicate the adsorption threshold of a rigid rod ($L_p \rightarrow \infty$) from eq. (23).

$V(z)$ that only depends on the distance z to the absorbing surface at $z = 0$, $\mathcal{H} = \mathcal{H}_b + \mathcal{H}_{\text{ad}}$. The adsorption potential is an attractive short-range square-well part V_a of range ℓ in front of a hard wall potential V_{wall} for a planar surface,

$$V(z) = V_a(z) + V_{\text{wall}}(z) = \begin{cases} \infty & \text{for } z < 0 \\ -g & \text{for } 0 < z \leq \ell \\ 0 & \text{for } z > \ell. \end{cases} \quad (2)$$

The potential strength $g > 0$ is an energy per length. Using this model, we can study adsorption both in $D = 2$ and $D = 3$ spatial dimensions. The persistence length of the semiflexible polymer as defined from the tangent-correlations of a free polymer is $L_p = 2\kappa/(D-1)k_B T$ [37] (note that the definition $L_p = 2\kappa/k_B T$ has been used in Refs. 5, 21, 23, 38, 39, whereas $L_p = \kappa/k_B T$ was used in Ref. 26). In the weak bending approximation (valid for $L, \xi < L_p$), we switch to the Monge parametrization with $\mathbf{r}(x) = (x, y(x), z(x))$ and rewrite the energies as $\mathcal{H}_b[z(x)] = \int_0^L dx \frac{\kappa}{2} (\partial_x z)^2$ and $\mathcal{H}_{\text{ad}}[z(x)] = \int_0^L dx V(z(x))$.

For the simulation, we discretize the semiflexible polymer into N beads connected by harmonic springs with a spring constant k and a bending energy derived from the bending angle of three neighboring beads with a bending rigidity κ [38]. In the simulations, this semiflexible harmonic chain is a phantom chain with no additional hard-core interactions between beads, i.e., there is no explicit

self-avoidance (as opposed to simulations in Ref. 27) but self-avoidance will be effectively fulfilled on length scales below L_p because of the bending energy. The discretization introduces another length scale into the simulation, which is the rest length b of the harmonic bonds resulting in an equilibrium contour length

$$L = (N - 1)b. \quad (3)$$

Discretization also affects the actual persistence length, which becomes [40]

$$L_{p,\text{dis}} = \frac{b}{\ln \left(I_{D/2-1} \left(\frac{\kappa}{bk_B T} \right) / I_{D/2} \left(\frac{\kappa}{bk_B T} \right) \right)} \quad (4)$$

where $I_n(x)$ is the modified Bessel function. For $L_{p,\text{dis}}/b \gtrsim 2$ the persistence length $L_{p,\text{dis}}$ approaches the continuous worm-like chain result $L_p = 2\kappa/(D-1)k_B T$. In the following, we will use the result (4) as persistence length to analyze simulation data for discrete semiflexible polymers.

We perform Monte-Carlo (MC) simulations of the adsorption process using a Metropolis algorithm with bead displacement moves of single beads or segments of beads. Each MC sweep consists of N MC moves, where segments of successive beads are moved by a random vector of length v . The MC displacement v is determined before each simulation to realize an acceptance rate of about 50% (typical values are $v \simeq 0.05$). A typical MC simulation consists of 10^7 sweeps.

In order to avoid that the polymer eventually diffuses away from the adsorbing plane to infinity one has to confine the polymer to the adsorbing plane. For the analysis of finite size effects in the adsorption transition it will turn out to be relevant how this confining mechanism is chosen, in particular, for finite stiff polymers with $L_d > L$. We use an end-grafting procedure and attach one end of the polymer to the boundary of the attractive potential, i.e., at $z = \ell$, in order to suppress diffusive motion of the polymer center of mass in the desorbed phase [27]. Confinement by end-grafting turns out to be convenient for the calculation of finite size effects in the rigid rod and stiff limit because it eliminates global translation of the chain and only allows for global rotation. Another choice is to confine the polymer by two hard walls as in Ref. 5, which allows for both global translation of the chain and global rotation between the confining walls.

Typical simulated polymers consist of several hundreds of beads. In the simulation we measure lengths in units of the bond length b and energies in units of $k_B T$. We use values $k = 100 k_B T / b^2$ or $k = 1000 k_B T / b^2$, for the harmonic spring stiffness to mimic a practically inextensible polymer. We change the persistence length L_p via the stiffness κ to explore finite size effects as a function of the dimensionless stiffness parameter L_p / ℓ .

The bond length has to be sufficiently small to avoid discretization effects. In the semiflexible regime $L_p > \ell$, a firmly adsorbed polymer decays into independently fluctuating segments of the size of the deflection length $L_d \sim L_p^{1/3} \ell^{2/3}$ by collisions with the potential boundary [30, 35, 36]: thermal fluctuations of a weakly bent free semiflexible polymer of length L are $\langle z^2 \rangle(L) \sim L^3 / L_p$, and the collision condition $\langle z^2 \rangle(L_d) \sim \ell^2$ determines the scaling of L_d . Therefore, the simulation exhibits discretization effects if $b > L_d$ because these collisions form fluctuations within the adsorption potential layer can no longer be properly resolved. This implies a choice $(L_p/b)^{1/3} (\ell/b)^{2/3} > 1$ or $(L_p/\ell)^{1/3} (\ell/b) > 1$ to avoid discretization effects for $L_p > \ell$. Note that also lattice simulation such as in Ref. 27 often represent the potential range by a single layer of adhesive sites effectively corresponding to a contact potential $\ell \ll b$ and can, therefore, not resolve any fluctuations within the adsorption potential layer.

In the flexible regime $L_p < \ell$ on the other hand, the polymer can be regarded as flexible polymer with an effective bond length of $2L_p$ also inside the potential well. Then discretization effects occur if $b > 2L_p$ if turns of the polymer can no longer be resolved properly. This implies a choice $2L_p/b > 1$ to avoid discretization effects for $L_p < \ell$.

III. CRITICAL POTENTIAL STRENGTH OF INFINITE POLYMERS

It is useful to first summarize known results for the adsorption transition of quasi-infinite semiflexible poly-

mers ($\xi < L$). They desorb by their internal configuration fluctuations, which can be envisioned as formation of desorbed loops and tails. The maximally accessible desorbed loop and tails size is limited by the correlation length ξ . All fluctuations on scales $< L_p$ are governed by bending energy of a semiflexible polymer, whereas fluctuations on scales $\gg L_p$ can be regarded as fluctuations of a flexible polymer with an effective bond length of $2L_p$.

A. Semiflexible regime

Infinite semiflexible polymers desorb by internal configuration fluctuations. If the persistence length exceeds the correlation length, $L_p \gtrsim \xi$, the desorbed “loops” are actually oriented segments without turns. If the persistence also exceeds the potential range ℓ , $L_p \gtrsim \ell$, the adsorbed tail segments cannot perform turns within the potential range. Then we are in the stiff or semiflexible limit of adsorption, where the critical potential strength is

$$g_{c,SF} = c_{SF} \frac{k_B T}{\ell} \left(\frac{L_p}{\ell} \right)^{-1/3} \quad (L_p \gtrsim \ell). \quad (5)$$

The exact exponent 1/3 occurring in eq. (5) has been obtained using different approaches: This result has been derived in Ref. 12 via the necklace model approach [28]. It has also been obtained explicitly in Refs. 2, 20, 21 by scaling arguments [2] or analytical transfer matrix calculations [20, 21]. Refs. 23, 26 (see also Supplemental Material of both Refs.) contain a more detailed account of analytical transfer matrix calculations of this result. In Ref. 26 (and Supplemental Material of 26), there are also results for the numerical prefactor

$$c_{SF} = 2^{-2/3} 3^{-1/3} \Gamma(1/3) (D-1)^{-1/3} \simeq 0.93 \left(\frac{2}{D-1} \right)^{1/3} \quad (6)$$

in eq. (5) (remember the different definition $L_p = \kappa / k_B T$ used in Ref. 26). In Ref. 5 the exponent 1/3 in the result (5) has been “rediscovered” ignoring all of these previous explanations.

The scaling with an exponent 1/3 in the result (5) for the critical potential strength is directly related to a corresponding scaling dependence of Odijk’s deflection length $L_d \sim L_p^{1/3} \ell^{2/3}$. This relation is established by a standard statistical mechanics argument: Confinement to the potential well costs entropy of the order of $1k_B$ per collision with the potential boundary, which gives a free energy cost per length $\Delta f = T \Delta s = k_B T / L_d$. Balancing this with the energy gain g per length gives the scaling of the adsorption threshold $ad g_c \sim k_B T / L_d$ resulting in eq. (5).

As a consequence, lattice simulations that cannot resolve fluctuations within the potential layer due to discretization effects, such as in Ref. 27, will find a different scaling behavior of the adsorption threshold, which is

dominated by discretization effects. A semiflexible lattice polymer will change lattice direction on its persistence length L_p on average. If the adsorption layer is a single layer of adhesive sites, confinement to this layer suppresses a finite fraction of configuration on the lattice every persistence length L_p , which leads to an entropy cost $T\Delta s \sim k_B T/L_p$ per length and, thus, to an adsorption threshold $g_c \sim k_B T/L_p$ as it was observed in Ref. 27.

In Ref. 23 it has been pointed out that the result (5) for the critical potential strength remains valid also if $L_p < \xi$ because it represents the critical potential strength to adsorb single segments of size L_p . In fact, the result (5) holds as long as these segments are larger than the potential range ℓ , $L_p \gg \ell$ [25, 26]. Then the semiflexible polymer is sufficiently rigid that loop formation of adsorbed trains inside the adsorption potential remain suppressed.

B. Flexible regime

The semiflexible result eq. (5) is applicable if L_p is larger than the potential range ℓ [25, 26]. For $L_p \lesssim \ell$, the polymer is in the flexible regime, where it can perform turns within the potential range. As it has been observed and analyzed in Refs. 25, 26, there is a maximum in the critical potential $g_c \ell$ for $L_p/\ell \sim 1$, such that adsorption becomes easier again in the flexible limit $L_p \lesssim \ell$, where

$$g_{c,F} = c_F \frac{k_B T L_p}{\ell} \quad (L_p \lesssim \ell) \quad (7)$$

is found with $c_F = 2\pi^2/4D(D-1)$ in D spatial dimensions in the absence of self-avoidance. The result (7) is the standard result $g_{c,F} \sim k_B T b/\ell^2$ for a flexible ideal chain [6] with effective bond length $b = 2L_p$. Again, lattice simulations can only find such a scaling behavior if the potential range is represented by several lattice spacings [41].

C. Crossover between regimes

In Ref. 26, the interpolation formula

$$\frac{g_c \ell}{k_B T} = I\left(\frac{L_p}{\ell}\right) \quad (8)$$

$$I(x) = c_1 x(1 + c_2 x^{4/3} + c_3 x^{2/3})^{-1} \quad (9)$$

has been derived, which describes both stiff and flexible limits and contains three free fit parameters c_1 , c_2 , and c_3 . The choices $c_1 = c_F$ and $c_2 = c_F/c_{SF}$ reproduce the analytically known flexible and semiflexible limits, and the remaining parameter c_3 allows to vary the position of the maximum to fit simulation data. In $D = 3$ we find best fits of our MC simulation data for parameter values as given in table II; these values slightly differ from results in Ref. 26 because we include discretization effects

data set	c_1/c_F	$c_2 c_{SF}/c_1$	c_3
theory (D=3)	1	1	free
cumulant	1.50 ± 0.05	1.03 ± 0.01	0.52 ± 0.06
finite size	1.08 ± 0.05	1.04 ± 0.02	0.74 ± 0.1
theory (D=2)	1	1	free
cumulant	1.05 ± 0.05	1.03 ± 0.01	0.00 ± 0.06
finite size	0.83 ± 0.05	1.05 ± 0.02	0.52 ± 0.1

TABLE II Simulation results for the fit parameters c_1 , c_2 , and c_3 for the interpolation function $I(x)$ from eq. (9) in comparison with theoretical expectations for $D = 3$ and $D = 2$. The adsorption threshold is determined by the cumulant method (maximal adsorption energy fluctuations) or finite size scaling.

properly by using the persistence length eq. (4); this improves the fit to the simulation data for small $L_p/b \lesssim 2$.

The MC data in Fig. 1 confirms that long polymers approach these results for infinite polymers. The data also shows pronounced finite size effects and a third adsorption regime in the stiff rod limit, which we will address below.

IV. THEORY OF LOOPS AND TAILS

A. Return exponents

Before discussing the adsorption of finite polymers it is useful to understand how the diverging correlation length ξ governs the length distribution of desorbed loops and tails of a semiflexible or flexible polymer. The length distributions of loops and tails has been examined recently in simulations [5, 27], where it was found that stiffer semiflexible polymers tend to desorb from their end by increasing tail lengths.

We want to explain the observations in Refs. 5, 27 using results from transfer matrix approaches and necklace models based on the grand canonical partition sum [9, 41, 42] (see Ref. 28 for a review on necklace models). The relevant quantity characterizing the size distribution of loops is the return or loop exponent χ , which determines the probability $p_{\text{return}} \sim L^{-\chi}$ for a *free* polymer starting in the attractive region of the potential well to return to this region for the first time as a function of its (projected) length L in the large L limit. The first return or loop exponent χ determines the critical properties of the adsorption transition. This can be seen in the necklace model approach, where the grand canonical partition sum is written as alternating series of bound (train) segments and loop segments. For polymer adsorption, we need the exponent χ for first returns to the attractive potential well at $0 < z < \ell$ in front of a hard wall.

In the following we distinguish between unconditioned returns, for which we use an exponent $\tilde{\chi}$, and first returns, for which we use the exponent χ . There is the general

relation

$$\chi = \max(2 - \tilde{\chi}, \tilde{\chi}) \quad (10)$$

between unconditional and first returns, which holds both for flexible and semiflexible chains and which can be derived, for example, using generating functions and the necklace representation [28].

For a flexible polymer without self-avoidance, the unconditioned return exponent in the absence of a wall is the standard result $\tilde{\chi}_{\text{RW}} = D/2$ for the return of Gaussian chains or random walks in D dimensions to the origin (starting point). For the adsorption of Gaussian chains this result is applied to a single dimension ($D = 1$), namely the z -coordinate of the polymer contour, which has to return to the potential well at $0 < z < \ell$, and with the arclength s as time-like coordinate of the random walk: $p_{\text{return}} \sim L^{-1/2}$ is the probability that the z coordinate returns to the adsorbing state $z \approx 0$ after length $s = L$, i.e., $\tilde{\chi}_{F,0} = 1/2$ in the absence of the hard wall at $z = 0$. In front of a hard wall, introduction of an image walker leads to a return exponent $\tilde{\chi}_F = 3/2$ for flexible polymers or random walks. This also follows from the observation that for flexible chains returns in front of a hard wall are equivalent to first returns in the absence of a hard wall such that, according to (10), $\chi_F = \tilde{\chi}_F = 2 - \tilde{\chi}_{F,0} = 3/2$.

The unconditioned return exponent for the weakly bent semiflexible phantom polymer to the adsorption potential in the presence of a hard wall is $\tilde{\chi}_{SF} = 5/2$ for return with orientation parallel to the wall. This is a non-trivial result which derives from an Ornstein-Uhlenbeck process and models a random walker with inertia, i.e., with random acceleration in 1 spatial dimension [29] (for semiflexible polymers returns in the presence of a hard wall are not equivalent to first returns in the absence of a wall because of additional restrictions on tangent vectors from the hard wall). For the adsorption problem this result is applied to the z -coordinate of the polymer contour and with the projected length x along the preferred orientation of the weakly bent semiflexible polymer as time-like coordinate of the inertial random walk: $p_{\text{return}} \sim L^{-5/2}$ is the probability that the z -coordinate returns to the adsorbing state $z \approx 0$ in parallel orientation $\partial_x z = 0$ after the projected length $x = L$ and in the presence of a hard wall at $z = 0$. The corresponding exponent for return irrespective of orientation is $\tilde{\chi}_{SF} = 2$ as integration over tangents always gives an additional factor $L^{1/2}$ reducing the exponent [39].

Alternatively, the exponents $\tilde{\chi}_F = 3/2$ and $\tilde{\chi}_{SF} = 5/2$ follow from the exponent relation $\tilde{\chi} = 1 + \nu_R$ [43], which holds in $D = 1$ dimensions (i.e., for returns in the z -coordinate) and in which ν_R is the exponent characterizing the end-to-end distance $\langle R^2 \rangle \sim L^{2\nu_R}$ and, thus, also the roughness in the z -coordinate $\langle z^2 \rangle \sim L^{2\nu_R}$. For semiflexible polymers $\nu_{R,SF} = 3/2$ resulting in $\tilde{\chi}_{SF} = 5/2$; for flexible phantom polymers $\nu_{R,F} = 1/2$ resulting in $\tilde{\chi}_F = 3/2$.

Using the relation (10) between unconditioned and first

returns we see that for adsorption in front of a hard wall, as considered here, return and first return (loop) exponents are identical and

$$\begin{aligned} \chi_F &= \tilde{\chi}_F = 3/2, \\ \chi_{SF} &= \tilde{\chi}_{SF} = 2. \end{aligned} \quad (11)$$

Loop or first return exponents are also known for self-avoiding chains, where

$$\chi_{\text{SAW}} = \begin{cases} 1 - \gamma_{11} \simeq 1.39 & \text{in } D = 3 \\ 19/16 = 1.1875 & \text{in } D = 2 \end{cases} \quad (12)$$

holds for returns of self-avoiding chains to a short-range adsorption potential in front of a hard wall [42, 44, 45]. Note that these result are close but not identical to the naive estimate $p_{\text{return}} \sim L^{-\nu_R}$ or $\tilde{\chi}_{\text{SAW},0} = \nu_{R,\text{SAW}}$ using the exponent ν_R of the end-to-end distance $\langle R^2 \rangle \sim L^{2\nu_R}$ and assuming that return in the z -coordinate is simply governed by the extension of the polymer, $p_{\text{return}} \sim 1/\langle R^2 \rangle^{1/2}$. Assuming also that returns in front of a hard wall are equivalent to first returns in the absence of a hard wall, we have $\tilde{\chi}_{\text{SAW}} = 2 - \tilde{\chi}_{\text{SAW},0} \simeq 2 - \nu_{R,\text{SAW}}$ according to (10). The Flory estimate $\nu_{R,\text{SAW}} = 3/(D+2)$ for self-avoiding polymers gives $\nu_{R,\text{SAW}} = 3/5$ in $D = 3$, more exact field-theoretical calculations give $\nu_{R,\text{SAW}} \simeq 0.588$ [46]; $\nu_{R,\text{SAW}} = 3/4$ is exact in $D = 2$ [45]. The reason for deviations from these naive estimates in eq. (12) are additional correlations between the z -component of the walk and components parallel to the surface by self-avoidance. Interestingly, in Ref. 42 it was shown that additional self-avoidance interactions between different adsorption loops exactly restore the naive result such that

$$\tilde{\chi}_{\text{SAW}} = 2 - \nu_{R,\text{SAW}} = \begin{cases} \simeq 1.41 & \text{in } D = 3 \\ = 1.25 & \text{in } D = 2. \end{cases} \quad (13)$$

According to (10), also for self-avoiding chains, return and first return exponents are identical in front of a hard wall, i.e., $\chi_{\text{SAW}} = \tilde{\chi}_{\text{SAW}} = 2 - \tilde{\chi}_{\text{SAW},0}$.

We note that, comparing loop exponents for flexible, self-avoiding and semiflexible polymers, we find $\chi_{\text{SAW}} < \chi_F < \chi_{SF}$ (see (11) and (13)), i.e., the exponent is smallest for the self-avoiding chain, although the exponents ν_R for the end-to-end distance are ordered differently, $\nu_{R,F} < \nu_{R,\text{SAW}} < \nu_{R,SF}$ (see (15)).

B. Order of adsorption transition

Necklace model [28] and transfer matrix approaches [39] independently show that the return exponent χ determines all other critical exponents of the adsorption transition. In particular, there is a relation between the first return exponent χ and the correlation length exponent ν of the adsorption transition ($\xi \propto |g - g_c|^{-\nu}$), which is

$$1/\nu = \min(\chi - 1, 1) \quad (14)$$

(correcting an error in Ref. 39). This relation gives

$$\begin{aligned} \nu_F &= 2, \\ \nu_{\text{SAW}} &= \frac{1}{1 - \nu_R} = \begin{cases} \simeq 2.43 & \text{in } D = 3 \\ = 4 & \text{in } D = 2. \end{cases} \\ \nu_{SF} &= 1 + \log \end{aligned} \quad (15)$$

from (11) [21, 23, 39] and (12).

For the adsorption transition, transfer matrix theory shows that the exponent ν is identical to the free energy exponent describing the singular part of the adsorption free energy density $|f_{\text{ad}}| \sim k_B T / \xi \propto |g - g_c|^\nu$ [21, 28] (i.e. hyperscaling holds). Thus, also the nature of the phase transition is entirely determined by the first return or loop exponent χ : If $\chi < 1$ the polymer is always bound for arbitrary weak potential; this case is not possible for a first return probability as immediately follows from the above relation (10). If $\chi > 1$ a threshold potential strength is necessary for adsorption. For $1 < \chi < 2$ or $\nu = 1/(\chi - 1) > 1$ the transition is continuous. For $\chi > 2$ or $\nu = 1$ the transition becomes discontinuous. So $\chi = 2$ and $\nu = 1$ marks the boundary between a discontinuous and continuous transition. The semiflexible polymer with $\chi_{SF} = 2$ is at this boundary and is weakly second order with $\nu_{SF} = 1 + \log$ as closer inspection shows [21]. Both flexible and self-avoiding chains have $1 < \chi_F, \chi_{\text{SAW}} < 2$ such that adsorption is continuous.

If the persistence length is small compared to the correlation length, $L_p < \xi$, there is a crossover in the critical properties, i.e., the critical exponents of the adsorption transition, to those of a flexible polymer, eventually a flexible self-avoiding chain. Because the correlation length $\xi \sim k_B T / |f_{\text{ad}}|$ ultimately diverges at the transition, the critical properties observable right at the adsorption transition should *always* be those of flexible chains with $\nu_F = 2$ or $\nu_{\text{SAW}} = 1/(1 - \nu_R) \simeq 2.43$ in the presence of self-avoidance. For stiff polymers with large L_p this critical behavior is, however, only observable for $|g - g_c| < k_B T / L_p$ (because of $\nu_{SF} \approx 1$), i.e., very close to the critical point [23]. As long as $|g - g_c| > k_B T / L_p$, the transition should have *apparent* critical exponents from the semiflexible regime [26]. Only in the rigid rod limit $L_p \rightarrow \infty$, a truly discontinuous transition as predicted from the semiflexible criticality should be observable. This crossover in critical properties often causes confusion, see for example a recent discussion in Ref. 27.

C. Finite size scaling results for critical properties

In principle, the correlation length or free energy exponent ν can be determined by finite size scaling of the adsorbed length $\langle L_{\text{ad}} \rangle = -\langle \mathcal{H}_{\text{ad}} \rangle / g$ or its second cumulant $C_{\text{ad}} \equiv \langle L_{\text{ad}}^2 \rangle - \langle L_{\text{ad}} \rangle^2$. Because $C_{\text{ad}} = -k_B T L \frac{\partial^2 f_{\text{ad}}}{\partial g^2}$ and $|f_{\text{ad}}| \sim k_B T / \xi \propto |g - g_c|^\nu$, we have $C_{\text{ad}} \propto L |g - g_c|^{\nu-2} \propto L \xi^{-1+2/\nu}$, which results in a finite size scaling

$$C_{\text{ad}} = L^{2/\nu} f((g - g_c)L^{1/\nu}) \quad (16)$$

for $g > g_c$ with a scaling function $f(x)$. This type of standard finite size scaling applies if the polymers are long enough to avoid the crossover to the additional rigid rod finite size corrections which will be discussed below in Sec. V.

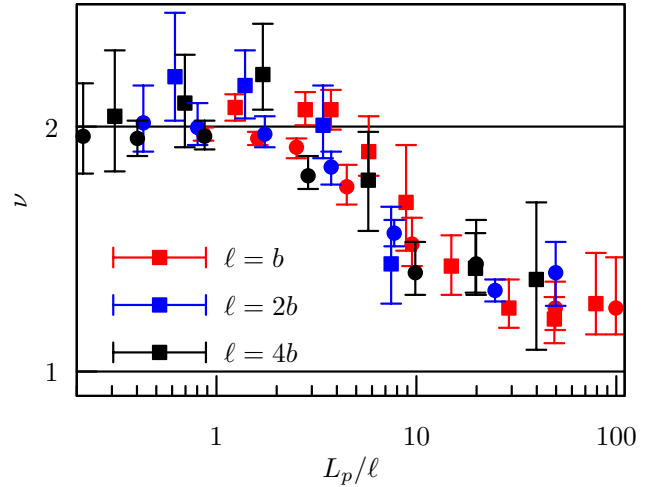


FIG. 2 Finite size scaling results for the exponent ν in $D = 2$ (squares) and $D = 3$ (circles) and for $\ell = b$ (red), $\ell = 2b$ (blue), $\ell = 4b$ (black) as a function of the stiffness parameter L_p/ℓ . Polymer lengths used in finite size scaling are $N = 50 - 800$, i.e., polymers are long enough to avoid the crossover to the rigid rod regime discussed in Sec. V.

An analysis of simulation data (see also 26 and Supplemental Material of 26 for more details) shows that the critical exponent measured by this approach indeed changes from $\nu \approx \nu_F = 2$ for $L_p/\ell < 1$ to $\nu \approx \nu_{SF} = 1$ for $L_p/\ell > 10$, see Fig. 2. The contour lengths and potential ranges used for finite size scaling in Fig. 2 are $L/b = 50 - 800$ and $\ell/b = 1 - 4$, respectively (therefore, for $L_p/\ell < 100$ the deflection length $L_d \sim L_p^{1/3} \ell^{2/3}$ is small compared to the contour length, $L_d < 20b < L$, such that the rigid rod limit and corrections from global rotation degrees of freedom to be discussed below can be neglected). For infinite semiflexible polymers, the crossover to the critical properties of flexible polymer adsorption should happen for $\xi > L_p$. For finite semiflexible polymers this crossover should remain unobservable if $L \lesssim L_p < \xi$ because the finite polymer cannot explore the relevant fluctuation wavelengths $> L_p$. Fig. 2 shows, however, that the semiflexible criticality for $L_p/\ell > 10$ remains observable even if much longer contour lengths up to $L/L_p = 80$ are used for finite size scaling. This suggests that L has to be substantially larger than L_p in order to observe the flexible polymer criticality.

D. Loop size distribution

The loop size distribution takes the form

$$p_{\text{loop}}(l) \sim l^{-\chi} e^{-l/\xi}. \quad (17)$$

with the loop exponent χ from eq. (11). This loop size distribution as derived from transfer matrix or necklace models only holds for large loops l exceeding any microscopic scales set by, e.g., the potential range ℓ such as the deflection length $L_d \sim L_p^{1/3} \ell^{2/3}$, which acts like an effective segment length for a bound semiflexible polymer. Loops sizes are cut off exponentially at the correlation length ξ . The shape of the loop size distribution (17) including the exponential cut off by the correlation length follows from transfer matrix treatments of the problem [21, 39]. For a polymer segment of length l starting at $z = 0$ and ending at $z = 0$, the number of loop configurations (not touching the potential in between) is given by the restricted partition sum $Z_0(z, z', l)$ of a free polymer as $Z_0(0, 0, L) \sim l^{-\chi}$. For an adsorbed polymer, the transfer matrix treatment shows the relation $|f_{\text{ad}}| = k_B T / \xi$ between the free energy per length (relative to $f_0 = 0$ for the free polymer, $f_{\text{ad}} < 0$ in the adsorbed phase) and the correlation length ξ of the transition [21, 28, 39]. The total partition sum of the adsorbed segment is, thus, $Z_{\text{ad}}(l) = \exp(-f_{\text{ad}} l / k_B T)$. The probability to find a loop of size l is

$$p_{\text{loop}}(l) = \frac{Z_0(0, 0, L)}{Z_{\text{ad}}(l)}, \quad (18)$$

which is of the form (17) with $\xi = k_B T / |f_{\text{ad}}|$ ($f_{\text{ad}} < 0$).

From the larger return exponent $\chi_{SF} = 2$ as compared to $\chi_F = 3/2$ or $\chi_{\text{SAW}} \simeq 1.412$ (in $d = 3$), see eq. (11), it follows that the loop size distribution shifts its weight to smaller sizes for stiffer polymers. For $\chi \leq 2$, the mean loop size $\langle l \rangle_{\text{loop}} = (\int_0^\infty dl l p_{\text{loop}}(l)) / (\int_0^\infty dl p_{\text{loop}}(l))$ diverges with ξ as $\langle l \rangle_{\text{loop}} \sim \xi^{2-\chi}$ for $1 < \chi < 2$ and $\langle l \rangle_{\text{loop}} \sim \ln \xi$ for $\chi = 2$. For finite polymers with $L < \xi$ loop sizes are cut off at the polymer length L and we find $\langle l \rangle_{\text{loop}} \sim L^{2-\chi}$ for $\chi < 2$ and $\langle l \rangle_{\text{loop}} \sim \ln L$ for $\chi = 2$ accordingly. We conclude that loop sizes are much smaller for semiflexible polymers, where we only find a weak log-divergence close to desorption ($\chi_{SF} = 2$) as compared to flexible polymers ($\chi_F = 3/2$), where $\langle l \rangle_{\text{loop}} \sim L^{1/2}$ (for $L < \xi$). This has also been observed in Ref. 5 in simulations.

For increasing loop size l we expect to see a crossover from a semiflexible behavior with $\chi_{SF} = 2$ for loops $l < L_p$ to a phantom or self-avoiding flexible behavior for loops $l > L_p$. The result $\chi_{\text{SAW}} \simeq 1.412$ for the self-avoiding walk is in qualitative agreement with an exponent $\chi_{\text{SAW}} \simeq 1.3$ observed in simulations in Ref. 27 for the loop distribution of very long self-avoiding semiflexible chains $l > L_p$. In order to probe the regime $l > L_p$ for $l < \xi, L$, it is necessary to have $L, \xi \gg L_p$, which is the regime investigated in Ref. 27. Experimentally, the flexible or self-avoiding regimes should be accessible, for example, for long DNA-strands with $L \gg L_p \simeq 50\text{nm}$ close to their adsorption transition. For polymers with $L \lesssim L_p$ as for F-actin as investigated in Ref. 5 or also for microtubules we rather expect to see semiflexible behavior of adsorption loops.

The exponents $\chi_F = 3/2$ for flexible polymers and

$\chi_{SF} = 2$ for semiflexible polymers from eq. (11) are confirmed by our MC simulations of long polymers without self-avoidance as shown in Fig. 3.

E. Tail size distribution

The corresponding length distribution of desorbed tails follows from interpreting a tail as the beginning of a loop. Therefore the tail distribution follows from integrating over all possible completions to a loop of size $s > l$,

$$p_{\text{tail}}(l) = \int_l^\infty ds p_{\text{loop}}(s)$$

$$p_{\text{tail}}(l) \sim \begin{cases} l^{-(\chi-1)} \exp(-l/\xi), & \chi > 1 \\ l^{-\chi} \exp(-l/\xi), & \chi < 1 \end{cases} \quad (19)$$

resulting in a tail exponent $\chi_F - 1 = 1/2$ for flexible polymers, $\chi_{\text{SAW}} - 1 \simeq 0.412$ for self-avoiding flexible polymers (in $d = 3$), and $\chi_{SF} - 1 = 1$ for semiflexible polymers. The reduction of the exponent by one shows that tails are always much larger than loops at the adsorption transition where $\xi \rightarrow \infty$. Both become limited by ξ in the adsorbed phase. For the mean tail size $\langle l \rangle_{\text{tail}} = (\int_0^\infty dl l p_{\text{tail}}(l)) / (\int_0^\infty dl p_{\text{tail}}(l))$, we find $\langle l \rangle_{\text{tail}} \sim \xi$ for $1 < \chi < 2$ and $\langle l \rangle_{\text{tail}} \sim \xi / \ln \xi$ for $\chi = 2$. For finite polymers with $L < \xi$, the cutoff ξ is replaced by the length L as for loops. Both for flexible and semiflexible polymers of length L , tails are diverging as $\langle l \rangle_{\text{tail}} \sim L$ with logarithmic corrections for semiflexible polymers.

Comparing loop and tail sizes, we conclude that both flexible and semiflexible polymers desorb by expanding tails over the whole polymer. Loop sizes at the transition are, however, significantly larger for flexible polymers. This explains the simulation results in Refs. 5, 27.

As for loops, we also expect for increasing tail sizes l to see a crossover from a semiflexible behavior with an exponent $\chi_{SF} - 1 = 1$ for loops $l < L_p$ to a flexible behavior for loops $l > L_p$ with $\chi_F - 1 = 1/2$ in the absence of self-avoidance and to $\chi_{\text{SAW}} - 1 = 1 - \nu_{R,\text{SAW}}$ for self-avoiding flexible polymers.

Fig. 3 shows our MC simulation results for the loop and tail distributions of long flexible polymers ($\kappa = 0$) and semiflexible polymers ($L_p/b \simeq 4000$, simulations in $D = 2$) without self-avoidance and with $N = L/b + 1 = 2000$ beads close to the transition such that the correlation length $\xi \lesssim L$ and loops and tails occur up to large sizes. We find $\chi_F = 1.487(2)$ and $\chi_{SF} = 1.85(1)$ in qualitative agreement with the theoretical result eq. (11). We determine the exponents χ and the corresponding correlations lengths ξ from fitting loop and tail distributions simultaneously and iteratively using eqs. (17) and (19): We first fit the tail distribution with ξ as fit parameter at fixed χ , then the loop distribution with fixed ξ and with χ as a fit parameter until ξ and χ converge. We omit small loop and tail size $l/b < 40$ for the fits (the potential range is $\ell = 0.1b$ such that $L_d \simeq 3.4$, i.e., only loops $l \gg L_d$ are considered).

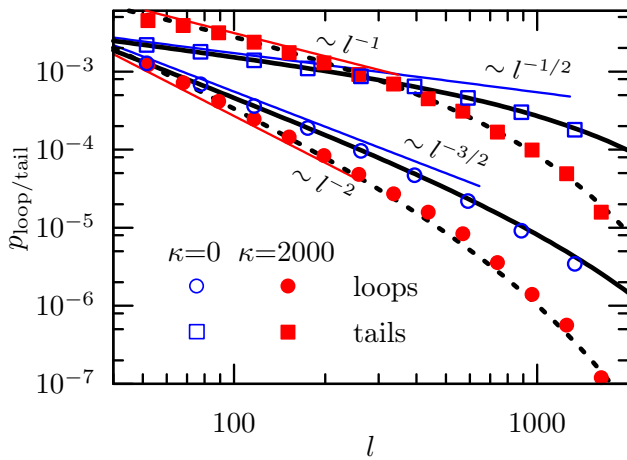


FIG. 3 Loop and tail size distributions for flexible ($\kappa=0$) and stiff polymers ($\kappa = 2000$). The expected power law behavior (see eqs. (17) and (19)) on intermediate length scales $b \ll l < \xi$ is marked as colored lines. We obtain return exponents $\chi_F = 1.487(2)$, $\chi_{SF} = 1.85(1)$ and correlation lengths $\xi_F/b = 1471(65)$ and $\xi_{SF}/b = 589(21)$ via an iterative fit scheme (see text).

F. Analyzing loop and tail distributions

The loop and tail distributions not only give insight into the desorption process and the differences between flexible and stiff polymers. The exponential cutoff $p_{\text{train}}(l) \propto \exp(-l/\xi)$ can also be used to determine the correlation length ξ and, thus, the free energy of adsorption via the relation $|f_{\text{ad}}| = k_B T/\xi$. The free energy of adsorption is otherwise difficult to determine experimentally.

Both loop and tail distributions (17) hold for loops l longer than the deflection length $L_d \sim L_p^{1/3} \ell^{2/3}$, which acts like an effective segment length for the bound trains in the model. Therefore, we propose to fit loop and tail distributions from simulations or experiments using eqs. (17) and (19) for $l > L_d$ using χ and $\xi = k_B T/|f_{\text{ad}}|$ as fit parameters. For simulations we performed such fits in Fig. 3.

We can also fit the experimental data of Ref. 5 on the tail distribution of actin filaments adsorbed by a depletion attraction. The quantity ζ from the simple exponential fit (eq. (1) in Ref. 5) should actually be the inverse correlation length $1/\xi$ and, thus, related to the free energy (per length) of adsorption by $\zeta = |f_{\text{ad}}|/k_B T$ (the experimental data does not allow to determine the exponent χ in (19)). We obtain free energies of adsorption as $|f_{\text{ad}}| \simeq 1.48, 8.76, 41.38 k_B T/L_p$ for the three data sets from Fig. 5 in Ref. 5 for depletant concentrations $C_p = 0.61, 0.65, 0.72$, see Fig. 4. The dependence on the reduced distance to the adsorption threshold $\gamma \equiv (\epsilon - \epsilon_m)/\epsilon_m = (C_p - C_{p,m})/C_{p,m}$ is governed by the exponent ν with $\nu_{SF} = 1 + \log$ for $\chi_{SF} = 2$, see eq. (15), i.e., $|f_{\text{ad}}| \propto \gamma/\ln|\gamma|$. The fit in Fig. 4 shows that the data for f_{ad} is consistent with this scaling law.

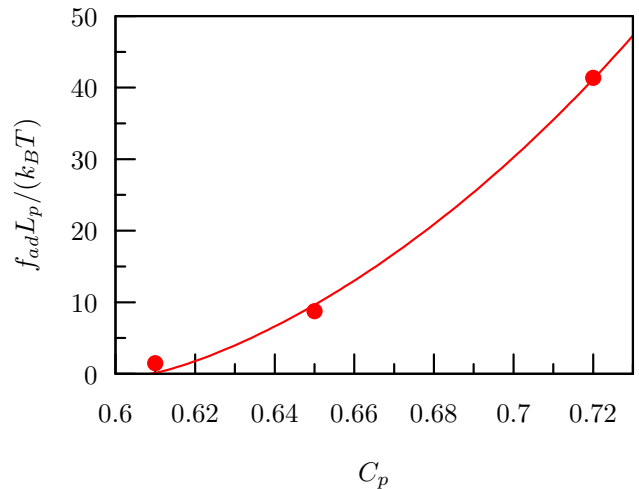


FIG. 4 Free energies of adsorption $|f_{\text{ad}}|$ (in units of $k_B T/L_p$) from the tail distribution data in Fig. 5 of the referred paper as a function of depletant concentration together with a fit $|f_{\text{ad}}| \propto \gamma/\ln|\gamma|$ (yielding $C_{p,m} = 0.61$ for the transition point).

V. CRITICAL POTENTIAL STRENGTH OF FINITE POLYMERS

We have shown that tail sizes diverge with the correlation length ξ upon approaching the desorption transition. Therefore, we expect finite size effects as soon as the correlation length exceeds the polymer length, $L < \xi$. According to the standard argument underlying finite size effects at a critical point, a polymer of finite length L should desorb easier, i.e., at larger g_c as soon as the correlation length ξ , which sets the scale for the desorbed tail length, reaches the polymer length L . In Ref. 41 it has been found that finite flexible lattice polymers have $g_c(L) > g_c$, i.e., finite polymers desorb easier only for narrow potentials corresponding to small $\ell \ll b$, whereas $g_c(L) < g_c$, i.e., finite polymers adsorb easier for wide potentials $\ell \gg b$. The latter effect is due to the large number of contacts with a wide attractive potential, which become more frequent for a short polymer if one end is grafted to the potential layer. Therefore, the direction of the finite size shift of $g_c(L)$ is a subtle issue that depends on the potential range ℓ . For desorption if ξ grows beyond L , finite size effects of the critical potential strength g_c are calculated according to $\xi(g_c) = L$, which corresponds to replacing the free energy criterion $f_{\text{ad}}(g_c) = 0$ by an apparent offset $f_{\text{ad}}(g_c) = k_B T/\xi(g_c) = -k_B T/L$. Because $\xi \propto |g - g_c|^{-\nu}$, this results in finite size corrections $g_c(L) - g_c \propto L^{-1/\nu}$, where the exponent ν is given by (15). This type of finite size corrections is the basis of the standard finite size scaling we employed above in eq. (16) and applies for sufficiently long polymers.

Finite size corrections have to be modified, however, for stiff or short polymers if the deflection length exceeds the polymer length, $L_d > L$. Then the polymer acts effectively as a rigid rod, and internal conformational fluctuations

tuations become negligible, whereas global rotation or translation degrees of freedom become relevant. These are additional fluctuation degrees of freedom, which tend to desorb the polymer leading to an *increase* in $g_c(L)$. In general, finite size corrections from a small number of global degrees of freedom can only be of the order of $g_c(L) - g_c \sim k_B T/L$ (eventually with logarithmic corrections). Therefore, this type of finite size correction is only relevant if $\nu \leq 1$, which is the case in the semiflexible and stiff limit where $\nu_{SF} = 1 + \log$, see eq. (15). For phantom flexible polymers with $\nu_F = 2$ or self-avoiding chains with $\nu_{SAW} \simeq 2.43$, on the other hand, finite size corrections from the diverging correlation length ξ are dominating. Therefore, we have to analyze finite size effects from global rotation and translation degrees of freedom in the rigid and semiflexible limit in the following.

A. End-grafted rigid rod

For a rigid rod, i.e., if $L_d/L \rightarrow \infty$, the result (5) for infinite polymers gives $g_{c,SF} \sim k_B T/L_d \approx 0$, i.e., an infinite rigid rod will adsorb for all $g > 0$ because all internal shape fluctuations and, thus, entropic costs of confinement to the potential well are suppressed in the rigid limit. We neglected, however, contributions from global translations and rotations of the rigid rod in the derivation of the adsorption threshold (5).

For finite rigid rods, adsorption is not a genuine phase transition because the rod has only $D - 1$ rotational (if the rod is axially symmetric) and D translational global degrees of freedom. Nevertheless, we can define a characteristic potential strength for adsorption either by the criterion that the adsorbed length $L_{ad} = -\mathcal{H}_{ad}/g$ exceeds half the polymer length[5], $\langle L_{ad} \rangle > L/2$, or by a maximum in the second cumulant $C_{ad} = \langle L_{ad}^2 \rangle - \langle L_{ad} \rangle^2$ of the adsorbed length.

A rigid rod with one end attached to the boundary of the attractive potential has only rotational degrees of freedom, and the adsorbed length can be calculated exactly. If θ is measured with respect to the positive z -axis, the polymer is out of the potential well for $0 < \theta < \pi/2$ and inside the potential well for a small angular interval $0 < \tilde{\theta} \equiv \pi/2 - \theta < \arcsin(\ell/L)$ resulting in ($\beta \equiv k_B T$)

$$Z_r = S_D/2 + S_{D-1} \int_0^{\arcsin(\ell/L)} d\tilde{\theta} \cos^{D-1} \tilde{\theta} e^{\beta g L} \quad (20)$$

$$\begin{aligned} F_r &= -k_B T \ln Z_r \\ &\approx -k_B T \ln \left(\frac{1}{2} S_D + S_{D-1} \frac{\ell}{L} e^{\beta g L} \right) \end{aligned} \quad (21)$$

and

$$\begin{aligned} \langle L_{ad} \rangle &= -\frac{\partial F_r}{\partial g} = \frac{L}{1 + \frac{S_D}{2S_{D-1}} \frac{\ell}{L} e^{-\beta g L}} \\ C_{ad} &= -k_B T \frac{\partial^2 F_r}{\partial g^2} = L^2 \frac{\frac{S_D}{2S_{D-1}} \frac{\ell}{L} e^{-\beta g L}}{\left(1 + \frac{S_D}{2S_{D-1}} \frac{\ell}{L} e^{-\beta g L} \right)^2} \end{aligned} \quad (22)$$

where $S_D = 2\pi^{D/2}/\Gamma(D/2)$ is the surface of the unit sphere in D dimensions, i.e., $S_3 = 4\pi$, $S_2 = 2\pi$, and $S_1 = 2$ (and $\beta \equiv k_B T$). Both the adsorption criterion $\langle L_{ad} \rangle > L/2$ and the maximum of the second cumulant C_{ad} agree and give

$$g_{c,rod}(L) = \frac{k_B T}{L} \ln \left(\frac{S_D}{2S_{D-1}} \frac{L}{\ell} \right) \quad (23)$$

with $S_3/2S_2 = 1$ in $D = 3$ and $S_2/2S_1 = \pi/2$ in $D = 2$. From the derivation starting from the partition sum (20) we see that $g_{c,rod}(L)$ can also be re-written in terms of the ratio of the accessible phase space volumes $Z_{r,0} = S_D/2$, where $\mathcal{H}_{ad} = 0$ and no potential acts, and $Z_{r,g} = S_{D-1} \frac{\ell}{L} e^{\beta g L}$, where the adsorption potential acts:

$$g_{c,rod}(L) = \frac{k_B T}{L} \ln (Z_{r,0}/Z_{r,g}(L)). \quad (24)$$

It is important to note that $g_{c,rod} \approx 0$ for $L \rightarrow \infty$, i.e., desorption of a rigid rod by global rotation fluctuations is only possible for finite rods. For a rigid rod, $g_{c,rod}(L)$ can also be interpreted as the finite size corrections to the infinite rod result $g_{c,SF} \approx 0$.

MC simulation results in Fig. 1 confirm that the adsorption threshold of finite polymers indeed exhibits pronounced finite size effects in the stiff limit and approaches $g_{c,rod}(L) \sim (k_B T/L) \ln(L/\ell)$ from eq. (23) in the stiff limit.

B. Crossover to the semiflexible regime

Upon reducing the ratio L_d/L by reducing stiffness or increasing length the result (23) for a rigid rod should cross over to the result (5) for an infinite semiflexible polymer. Equating $g_{c,rod}(L) = g_{c,SF} \sim k_B T/L_d$ gives $L_d \sim L$ as crossover point. For $L_d > L$ we thus expect adsorption of a very weakly fluctuating almost rigid rod, whereas for $L > L_d$, there should be a crossover to the semiflexible result (5), for which collisions with the adsorption potential boundaries on the scale L_d are important. This crossover proceeds via three regimes upon reducing the stiffness and, thus, the deflection length $L_d \sim L_p^{1/3} \ell^{2/3}$ and the persistence length L_p ($L_d < L_p$ because $\ell \ll L_p$) or increasing the length L :

- (i) For large stiffness $L < L_d < L_p$ [or $N = L/b + 1 < (L_p/\ell)^{1/3}(\ell/b)$] an adsorbed rigid rod starts to bend by thermal fluctuations but will have typically no thermal collisions with the boundaries of the adsorption potential of range ℓ . Thermal fluctuations only give rise to a finite effective thickness $\langle z^2 \rangle^{1/2}$ of the rod. For an end-grafted rod this restricts the accessible rotation angles θ (Fig. 5).
- (ii) For reduced stiffness such that $L_d < L < L_p$ [or $(L_p/\ell)^{1/3}(\ell/b) < N < (L_p/\ell)(\ell/b)$], thermal fluctuations within the potential well are sufficient to

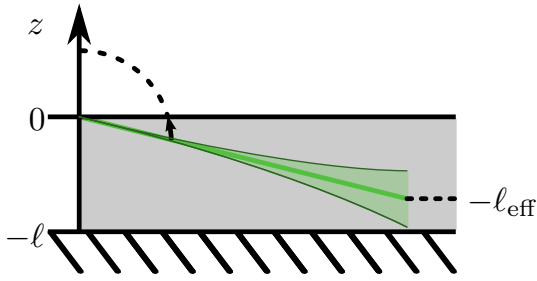


FIG. 5 Effective thickness $\ell_{\text{eff}} \approx \ell - cL^{3/2}/L_p^{1/2}$ of a stiff rod caused by thermal fluctuations.

induce repeated collisions with the boundaries of the adsorption layer which gives rise to an additional free energy cost per length.

- (iii) For $L_d < L_p < L$ [or $N > (L_p/\ell)(\ell/b)$], the length over which the orientation of the first segment grafted to the potential well can persist, which is by definition the persistence length L_p , becomes smaller than the polymer length L . Then the global rotation degree of freedom only affects a segment of length L_p .

- (i) For $L < L_d$, an adsorbed semiflexible polymer bends by thermal fluctuations with $\langle z^2 \rangle \sim L^3/L_p < \ell^2$ such that it typically has no thermal collisions with the boundaries of the adsorption layer of size ℓ . The fluctuations give the rigid rod, however, an increased effective thickness $\langle z^2 \rangle^{1/2}$, which restricts the range of rotation angles where the polymer fits without bending into the potential well to $0 < \theta - \pi/2 < \arcsin(\ell_{\text{eff}}/L)$ with a reduced effective width

$$\ell_{\text{eff}} = \ell - \langle z^2 \rangle^{1/2} \approx \ell - cL^{3/2}/L_p^{1/2}, \quad (25)$$

where c is a numerical prefactor (Fig. 5).

Using the effective potential width (25) in the rigid rod result (23) gives a T -dependent shift of the adsorption threshold,

$$g_c(L) = g_{c,\text{rod}}(L) + \frac{k_B T}{L} \ln \left(1 + c \frac{L^{3/2}}{L_p^{1/2} \ell} \right). \quad (26)$$

For $L \ll L_d$ we can expand the logarithm, and the shift becomes $g_c(L) - g_{c,\text{rod}}(L) \approx ck_B T L^{1/2}/L_p^{1/2} \ell \propto L_p^{-1/2}$.

- (ii) If $L_d < L < L_p$, thermal fluctuations are sufficient to induce repeated collisions with the boundaries of the adsorption potential. This increases the free energy f_{ad} per length of a polymer with $0 < \theta - \pi/2 < \arcsin(\ell/L)$ by an additional entropic contribution for the confinement to the potential well of width ℓ ,

$$f_{\text{ad}} \approx -g + ak_B T \frac{1}{\ell^{2/3} L_p^{1/3}}. \quad (27)$$

This contribution stems from restricting the internal shape fluctuations. The prefactor of the confinement free energy has been measured in simulations as $a \simeq 1.1$ [32] for a hard confinement to a width ℓ , which should be appropriate for large $g \gg g_c$. At $g = g_{c,SF}$ the free energy f_{ad} should vanish; this suggests $a = c_{SF}$ with c_{SF} as in (6) in the vicinity of the transition. Both $a \simeq 1.1$ for $g \gg g_c$ and $a = c_{SF}$ for $g \approx g_c$ are comparable and of order unity. The estimate (27) is also compatible with an exponent $\nu = 1$ of the adsorption free energy $|f_{\text{ad}}| \sim k_B T/\xi \propto |g - g_{c,SF}|^\nu$ close to the transition, i.e., with neglecting the logarithmic correction in $\nu = \nu_{SF} = 1 + \log$, see eq. (15). Therefore, we can approximate the partition sum of the internal deformation degrees of freedom of an adsorbed semiflexible polymer by $Z_i(L) = e^{-\beta f_{\text{ad}} L}$, which replaces the rigid rod Boltzmann factor $e^{\beta g L}$.

Replacing g in the free energy (21) of a rigid rod by the adsorption free energy f_{ad} results in a critical potential strength for a finite semiflexible polymer

$$\begin{aligned} g_c(L) &= g_{c,\text{rod}}(L) + ak_B T \frac{1}{\ell^{2/3} L_p^{1/3}} \\ &= g_{c,\text{rod}}(L) + g_{c,SF}. \end{aligned} \quad (28)$$

This result holds *independently* of the adsorption criterion ($\langle L_{\text{ad}} \rangle(g_c) = L/2$ or based on the second cumulant). The critical potential strength (28) can be interpreted in two ways: first as the rigid rod result (23), which is shifted by an offset identical to the semiflexible result $g_{c,SF}$ from eq. (5). Therefore, the temperature-induced shift with respect to the rigid rod result scales as $g_c(L) - g_{c,\text{rod}}(L) \propto L_p^{-1/3}$, in the regime $L < L_d$, which differs from the scaling $g_c(L) - g_{c,\text{rod}}(L) \propto L_p^{-1/2}$ for $L > L_d$, see Fig. 6. Second as the as the semiflexible result $g_{c,SF}$ from eq. (5) for an infinite polymer, which is shifted by finite size corrections due to the global rotation degree of freedom and given by the rigid rod result $g_{c,\text{rod}}(L) \propto L^{-1} \ln L$.

Additional finite size corrections arise from the internal shape fluctuations for $\xi > L$, which shift will also give a shift $\Delta g_c(L) \sim k_B T L^{-1} \ln L$ because $\nu = \nu_{SF} = 1 + \log$, see eq. (15). They correspond to an additional contribution $\pm k_B T L^{-1} \ln L$ to f_{ad} in eq. (27) from fluctuations in a finite size system. Therefore, we expect $g_c(L) = \alpha g_{c,\text{rod}}(L) + g_{c,SF}$ with a numerical prefactor α to the rigid rod correction to the semiflexible result $g_{c,SF}$ from eq. (5). Therefore, for $L_p < L < L_d$, it should be possible to find a numerical constant $\alpha \sim \mathcal{O}(1)$ such that $g_c(L) - \alpha g_{c,\text{rod}}(L) \sim g_{c,SF}$ collapses onto the length-independent infinite semiflexible polymer result $g_{c,SF}$ from eq. (5). Our simulation data in Fig. 6 is well described by $\alpha \simeq 0.5$ suggesting that finite size effects from internal fluctuations and from the

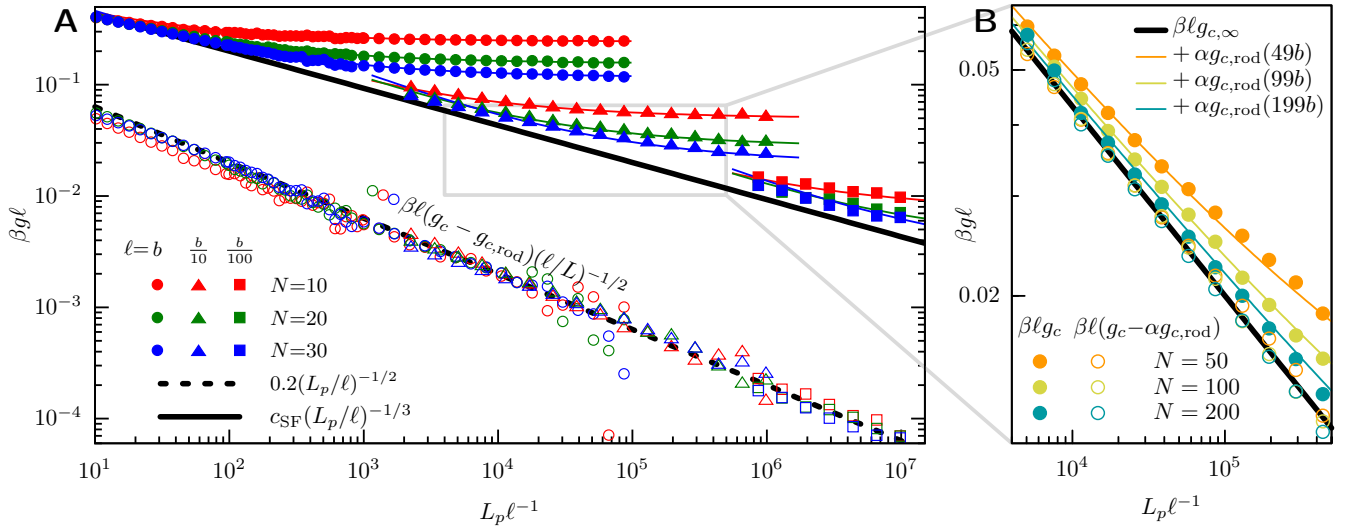


FIG. 6 Finite size effects for various potential widths ℓ and contour lengths for an end-grafted semiflexible polymer. For shorter chains ($N = L/b + 1 = 10, 20, 30$) finite size effects are best described by the rigid rod with an increased effective thickness using eq. (26) (**A** with $\ell/b = 1, 0.1, 0.01$), which allows data collapse onto one curve $\propto L_p^{-1/2}$. Longer chains ($N = L/b + 1 = 50, 100, 200$) are best described by the rigid rod with additional entropic free energy cost using eq. (28) (**B** with $\ell = 0.1b$). Subtracting $\alpha g_{c,\text{rod}}(L)$ (with $\alpha \approx 0.5$) from the measured critical potential strengths recovers the critical potential strength of the infinite chain. The crossover takes place when L becomes shorter than the deflection length L_d (for $L < (L_p/\ell)^{1/3}(\ell/b)$).

rigid rod degrees of freedom become comparable in this regime.

- (iii) If L_p is further reduced below L such that $L > L_p$, rotations of the first segment only affect the polymer over a persistence length L_p . Then the free energy is

$$F(L) = -k_B T \ln Z(L_p) + (L - L_p) f_{\text{ad}}$$

where $Z(L_p)$ is the partition sum of an end-grafted segment of length $L_p > L_d$ (as in regime (ii)) and f_{ad} is the adsorption free energy per length of the infinite polymer. The adsorbed length is given by $\langle L_{\text{ad}} \rangle = -\partial F / \partial g$ and using the criterion $\langle L_{\text{ad}} \rangle = L/2$ we obtain an adsorption threshold, which approaches for $L_p = L/2$ the semiflexible result $g_{c,SF}$ for an infinite polymer. Therefore, finite size effects from the global rotation degrees of freedom become irrelevant for $L_p < L/2$. Then we only expect small finite size effects from internal deformation degrees of freedom if $\xi > L$, which also scale as $\Delta g_c(L) \sim k_B T L^{-1} \ln L$ because $\nu = \nu_{SF} = 1 + \log$.

C. Semiflexible polymer confined by two hard walls

Alternatively, we can consider confinement by a second parallel non-adsorbing hard wall at a distance $L_z > \ell$ in order to avoid that the polymer diffuses away. This type of confinement has been considered in Ref. 5. For a completely rigid rod we calculate the ratio of the phase space

volumes $Z_{r,0}$, where $\mathcal{H}_{\text{ad}} = 0$, and $Z_{r,g}$, where the adsorption potential acts, and then apply eq. (24) as above for the end-grafted rod. Contrary to the end-grafted polymer, where the first bead is held fixed, the prefactor for a free polymer is $\propto 1/Nb$, since the potential acts on $N = (L + 1)/b$ beads, where the entropic confinement depends on the actual contour length $L = (N - 1)b$.

Now the rod can perform global rotations *and* translations. We parametrize global rotations by the angle θ (or $\tilde{\theta} \equiv \pi/2 - \theta$ with $0 < \theta, \tilde{\theta} < \pi/2$ for non-polar rods) and global translations by the coordinate z of the rod center (rotations within the adsorbing plane or translations parallel to the adsorbing plane play no role). The phase space volume $Z_{r,0}$ is (for $\ell \ll L_z$) simply the partition sum of a free rod between two walls with distance L_z , which is obtained from observing that only angles $0 < \tilde{\theta} < \arcsin(L_z/L)$ are possible and that, for a given angle $\tilde{\theta}$, only z -coordinates $z > (\sin \tilde{\theta})L/2$ and $z < L_z - (\sin \tilde{\theta})L/2$ are accessible,

$$Z_{r,0} = S_{D-1} \int_0^{\arcsin L_z/L} d\tilde{\theta} \cos^{D-1} \tilde{\theta} (L_z - L \sin \tilde{\theta}) \approx S_{D-1} \frac{L_z^2}{2L}. \quad (29)$$

Likewise, phase space volume $Z_{r,g}$ is approximately the partition sum of a polymer confined between two walls with separation ℓ , i.e., $Z_{r,g} \approx S_{D-1} \ell^2 / 2L$ resulting in

$$g_{c,\text{rod}}(L) = \frac{k_B T}{Nb} \ln(Z_{r,0}/Z_{r,g}(L)) \approx \frac{2k_B T}{Nb} \ln\left(\frac{L_z}{\ell}\right) \quad (30)$$

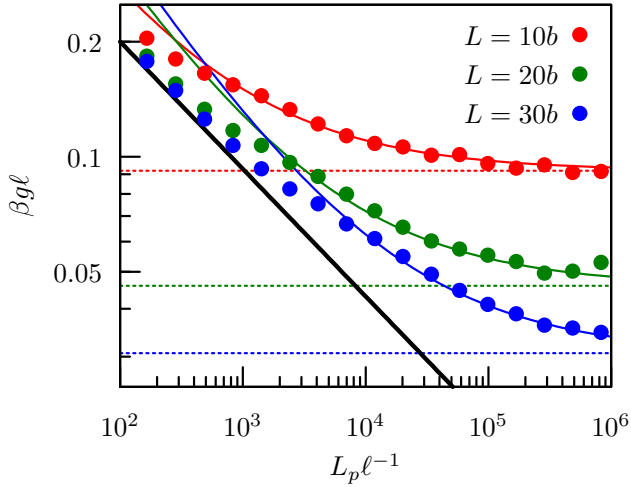


FIG. 7 (30) Finite size effects for a free semiflexible polymer (with $N = L/b + 1 = 10, 20, 30$) confined between two walls separated by a distance $L_z = 10b$. In front of one wall there is an attractive square-well potential with width $\ell = 0.1b$. The critical potential strength is best described by eq. (31) (solid curves), which shows the crossover from an infinite semiflexible chain (eq. (5), solid black line) to a rigid rod (eq. (30), dashed horizontal lines).

(which deviates by a factor of 2 from the result given in Ref. 5). MC simulation results in Fig. 7 confirm that the adsorption threshold of finite polymers between two hard walls indeed approaches $g_{c,\text{rod}}(L)$ from eq. (30) in the stiff limit.

For $L_z \sim L$ the result becomes similar to (23) for an end-grafted polymer. The global degrees of freedom involved in (30) are, however, rotations *and* translations, whereas they are only rotations for the end-grafted rod. Also corrections for finite temperatures are similar and go through the same three regimes for decreasing L_p .

- (i) For $L < L_d$ the polymer is a weakly fluctuating rigid rod with an increased effective thickness leading to an effectively decreased potential width ℓ_{eff} as in eq. (25). Using ℓ_{eff} in the rigid rod result (30) gives a T -dependent shift

$$g_c(L) = g_{c,\text{rod}}(L) + \frac{2k_B T}{L} \ln \left(1 + c \frac{L^{3/2}}{L_p^{1/2} \ell} \right), \quad (31)$$

which, for $L \ll L_d$ gives a shift $g_c(L) - g_{c,\text{rod}}(L) \sim k_B T L^{1/2} / L_p^{1/2} \ell \propto L_p^{-1/2}$ as for end-grafting.

- (ii) For $L_d < L < L_p$, there is an additional entropic free energy cost due to repeated collisions with the boundaries, see eq. (27). This leads to the same shift as in the end-grafting result (28).
- (iii) for $L > L_p$ the overall orientation of the polymer is lost and finite size effects only come from the global translational degree of freedom. If the size

of the polymer as measured by its end-to-end distance $\langle R^2 \rangle^{1/2}$ is of the order of L_z or larger, we do not expect finite size corrections from global translation. For $L_z > \langle R^2 \rangle^{1/2}$, finite size corrections from global translation will be of the order of $g_c(L) - g_{c,SF} \sim k_B T \ln(L_z / \langle R^2 \rangle^{1/2})$.

D. Finite size effects in the flexible limit

As discussed above, in the flexible regime $L_p \ll \ell$ finite size corrections from internal shape fluctuations result in a shift $|g_c(L) - g_c| \propto L^{-1/\nu}$ with $\nu = \nu_F = 2$ if $\xi > L$.

There is, however, an additional source of finite size corrections associated with a finite potential range ℓ . Upon decreasing L_p , the mean square radius $\langle R^2 \rangle \sim 2L_p L$ as given by the flexible chain result with an effective segment length of $b \approx 2L_p$ becomes smaller than the square of the potential range for $L < \ell^2 / 2L_p$. Then, the entire chain can accommodate into the potential well without entropic free energy costs resulting in $g_c \approx 0$ for $L < \ell^2 / 2L_p$. Therefore, in the flexible limit, the finite size result for g_c should approach the infinite polymer result $g_{c,F}$ from eq. (7) from below.

VI. FINITE SIZE SCALING PROCEDURE

Based on our results for the finite size corrections of the adsorption threshold, we obtain a method to analyze adsorption data for finite semiflexible polymers such as filamentous actin. We assume that the adsorption threshold $g_c(L)$ has been determined experimentally or in simulations for finite polymers and want to demonstrate how to fit to the theory presented above, which will allow us to extract possible fit parameters such as the persistence length L_p or the potential range ℓ .

Our above results in the semiflexible regime $L < L_p$ (eqs. (23), (26) for case (i) $L < L_d$ and eqs. (30), (31) for case (ii) $L_d < L < L_p$) show that global rotation and translational degrees of freedom play a dominating role for finite size corrections in this regime. In order to correct for these effects we can subtract the rigid rod result $g_{c,\text{rod}}(L)$ and continue with an analysis of the data for $g_c(L) - g_{c,\text{rod}}(L)$.

We then have to distinguish between case (i) $L < L_d$ and case (ii) $L_d < L < L_p$. In case (i) we fit the shifted data $g_c(L) - g_{c,\text{rod}}(L)$ according to (23) and (30) with $g_c(L) - g_{c,\text{rod}}(L) \sim k_B T L^{1/2} / L_p^{1/2} \ell$ for both end-grafting and wall-confinement. In case (ii) we fit the shifted data $g_c(L) - g_{c,\text{rod}}(L)$ according to (26) and (31) using $g_c(L) - g_{c,\text{rod}}(L) \sim g_{c,SF} \sim k_B T / \ell^{2/3} L_p^{1/3}$. In both cases, these fits should enable us to extract material parameters such as the persistence length L_p .

A similar fit procedure (using only case (ii)) has actually been used in Ref. 5 to analyze data but on phenomenological grounds. The arguments presented in this

paper systematically justify this technique and show the necessary distinction between case (i) of an essentially rigid rod for $L > L_d$ and case (ii) of a semiflexible polymer for $L_d < L < L_p$. In Ref. 5 the use of case (ii) was appropriate because the potential range ℓ and, thus, L_d was small.

VII. DISCUSSION AND CONCLUSION

In this paper we unraveled the different adsorption regimes for finite semiflexible polymers if persistence length L_p , potential range ℓ , and the finite contour length L are changed. An overview of all regimes is given in table I. Finite semiflexible polymers exhibit three distinct regimes for the adsorption potential strength: (i) a flexible or Gaussian regime if the persistence length is smaller than the adsorption potential range, (ii) a semiflexible regime if the persistence length is larger than the potential range, and (iii) for finite polymers, a novel crossover to a rigid rod regime if the deflection length exceeds the contour length.

Our main result is the novel adsorption regime (iii) for finite stiff polymers if the deflection length L_d exceeds the contour length, $L < L_d \sim L_p^{1/3} \ell^{2/3}$, see Fig. 1. Then the adsorption threshold is governed by the global rotational and translational degrees of freedom of a finite rigid rod. For end-grafted polymers we find in the rigid rod limit $g_{c,rod}(L) \sim (k_B T/L) \ln(L/\ell)$, see eq. (23). Upon reducing the stiffness or increasing the length, the threshold crosses over to the semiflexible regime with $g_{c,SF} \sim k_B T/L_d \sim k_B T/L_p^{1/3} \ell^{2/3}$ according to (5), which can be described by eq. (28). For adsorption in confinement between two walls we find analogous result, see Fig. 7. Based on our results we can derive a finite size scaling

procedure to analyze adsorption data on finite semiflexible polymers.

In Ref. 5 the adsorption of the semiflexible polymer F-actin has been studied recently. For F-actin contour and persistence lengths $L \sim L_p \sim 10 - 20 \mu\text{m}$ are typical. Depletion potentials in Ref. 5 have a range $\ell \sim 10\text{nm}$. Other possible attractive potentials are electrostatic interactions with $\ell \sim 1\text{nm}$ at physiological conditions for monovalent ions and larger ranges $\ell \propto 1/z\sqrt{c_{\text{salt}}}$ at lower salt concentrations or higher valencies z , which gives similar ranges as for depletion. Therefore, we are in the regime $L_d \ll L_p \sim L$ for F-actin experiments and the adsorption threshold should be described by the semiflexible result for an infinite polymer, $g_{c,SF} \sim k_B T/L_d \sim k_B T/L_p^{1/3} \ell^{2/3}$ according to (5). Only relatively small finite size corrections of the rigid rod form according to (28) should be observable according to our theory. This is in accordance with the results in Ref. 5.

The novel rigid rod regime with a pronounced length-dependence of the adsorption threshold (23) should be accessible, for example, for short microtubules. For a microtubule persistence length $L_p \sim 5\text{mm}$ and similar potential ranges $\ell \sim 10\text{nm}$ as for F-actin, we find $L_d \sim L \ll L_p$ for contour lengths $L \sim 1\mu\text{m}$.

Moreover, we presented a theory for the loop and tail distributions of flexible and semiflexible polymers and the critical exponents governing these distributions close to the adsorption threshold. Our results (17) for loops and (19) for tails explain that, close to the transition, semiflexible polymers have significantly smaller loops and both flexible and semiflexible polymers desorb by expanding their tail length. This agrees with simulation observations in Refs. 5, 27. The tail distribution allows us to directly extract the free energy per length of adsorption f_{ad} from the experimental data presented in Ref. 5, see Fig. 4.

-
- [1] J. Skolnick and M. Fixman, *Macromolecules* **10**, 944 (1977).
 - [2] R. R. Netz and J.-F. Joanny, *Macromolecules* **32**, 9013 (1999).
 - [3] A. Ott, M. Magasco, A. Simon, and A. Libchaber, *Phys. Rev. E* **48**, R1642 (1993).
 - [4] P. Venier, A. C. Maggs, M.-F. Carlier, and D. Pantaloni, *J. Biol. Chem.* **269**, 13353 (1994).
 - [5] D. Welch, M. P. Lettinga, M. Ripoll, Z. Dogic, and G. A. Vliegenthart, *Soft Matter* **11**, 7507 (2015).
 - [6] P. de Gennes, *Scaling Concepts in Polymer Physics* (Cornell University Press, Ithaca and London, 1979).
 - [7] E. Eisenriegler, *Polymers near Surfaces* (World Scientific, London, 1993).
 - [8] R. R. Netz and D. Andelman, *Phys. Rep.* **380**, 1 (2003).
 - [9] T. M. Birshstein, E. B. Zhulina, and A. M. Skvortsov, *Biopolymers* **18**, 1171 (1979).
 - [10] A. C. Maggs, D. A. Huse, and S. Leibler, *Europhys. Lett.* **8**, 615 (1989).
 - [11] G. Gompper and T. Burkhardt, *Phys. Rev. A* **40**, 6124 (1989).
 - [12] G. Gompper and U. Seifert, *J. Phys. A: Math. Gen.* **23**, L1161 (1990).
 - [13] A. R. Khokhlov, F. F. Ternovsky, and E. A. Zheligovskaya, *Makromol. Chem., Theory Simul.* **2**, 151 (1993).
 - [14] E. Kramarenko, R. Winkler, P. Khalatur, A. Khokhlov, and P. Reineker, *J. Chem. Phys.* **104**, 4806 (1996).
 - [15] C. C. van der Linden, F. A. M. Leermakers, and G. J. Fleer, *Macromolecules* **29**, 1172 (1996).
 - [16] D. V. Kuznetsov and W. Sung, *J. Chem. Phys.* **107**, 4729 (1997).
 - [17] R. Bundschuh, M. Lässig, and R. Lipowsky, *Eur. Phys. J. E* **3**, 295 (2000).
 - [18] T. Sintes, K. Sumithra, and E. Straube, *Macromolecules* **34**, 1352 (2001).
 - [19] S. Stepanow, *J. Chem. Phys.* **115**, 1565 (2001).
 - [20] A. N. Semenov, *Eur. Phys. J. E* **9**, 353 (2002).
 - [21] J. Kierfeld and R. Lipowsky, *Europhys. Lett.* **62**, 285 (2003).
 - [22] P. Benetatos and E. Frey, *Phys. Rev. E* **67**, 051108 (2003).

- (2003).
- [23] J. Kierfeld, Phys. Rev. Lett. **97**, 058302 (2006).
- [24] A. L. Owczarek, J. Stat. Mech. Theor. Exp. **2009**, P11002 (2009).
- [25] M. Deng, Y. Jiang, H. Liang, and J. Chen, J. Chem. Phys. **133**, 034902 (2010).
- [26] T. A. Kampmann, H.-H. Boltz, and J. Kierfeld, J. Chem. Phys. **139**, 034903 (2013).
- [27] H.-P. Hsu and K. Binder, Macromolecules **46**, 2496 (2013).
- [28] M. E. Fisher, J. Stat. Phys. **34**, 667 (1984).
- [29] T. Burkhardt, J. Phys. A: Math. Gen. **26**, L1157 (1993).
- [30] T. Odijk, Macromolecules **16**, 1340 (1983).
- [31] L. Harnau and P. Reineker, Phys. Rev. E **60**, 4671 (1999).
- [32] D. J. Bicout and T. W. Burkhardt, J. Phys. A: Math. Gen. **34**, 5745 (2001).
- [33] P. Kraikivski, R. Lipowsky, and J. Kierfeld, Eur. Phys. J. E **16**, 319 (2005).
- [34] P. Levi and K. Mecke, Europhys. Lett. **78**, 38001 (2007).
- [35] S. Köster, H. Stark, T. Pfohl, and J. Kierfeld, Biophys. Rev. Lett. **2**, 155 (2007).
- [36] S. Köster, J. Kierfeld, and T. Pfohl, Eur. Phys. J. E **25**, 439 (2008).
- [37] P. Gutjahr, R. Lipowsky, and J. Kierfeld, EPL **76**, 994 (2006).
- [38] J. Kierfeld, O. Niamploy, V. Sa-Yakanit, and R. Lipowsky, Eur. Phys. J. E **14**, 17 (2004).
- [39] J. Kierfeld and R. Lipowsky, J. Phys. A: Math. Gen. **38**, L155 (2005).
- [40] H. Kleinert, *Path integrals in quantum mechanics, statistics, polymer physics, and financial markets; 3rd ed.* (World Scientific, River Edge, NJ, 2004) based on a Course on Path Integrals, Freie Univ. Berlin, 1989/1990.
- [41] L. I. Klushin, A. A. Polotsky, H.-P. Hsu, D. A. Markelov, K. Binder, and A. M. Skvortsov, Phys. Rev. E **87**, 022604 (2013).
- [42] S. Bhattacharya, V. G. Rostiashvili, A. Milchev, and T. A. Vilgis, Macromolecules **42**, 2236 (2009).
- [43] R. Lipowsky, Zeitschrift für Physik B Condensed Matter **97**, 193 (1995).
- [44] P. Grassberger, J. Phys. A: Math. Gen. **38**, 323 (2005).
- [45] C. Vanderzande, *Lattice Models of Polymers*, Cambridge Lecture Notes in Physics (Cambridge University Press, 1998).
- [46] J. C. Le Guillou and J. Zinn-Justin, Phys. Rev. B **21**, 3976 (1980).